Critical current measurement in HTS Bi2212 ribbons and round wires

Jean-Michel Rey, Arnaud Allais, Jean-Luc Duchateau, Philippe Fazilleau, Jean-Marc Gheller, Ronan Le Bouter, Olivier Louchard, Lionel Quettier, Daniel Tordera

***Abstract*—Recent progresses in Bi2212 wires have proved its suitability for round wire developments and high field magnet insert manufacturing. In order to prepare cabling developments the Commissariat à l'Energie Atomique at Saclay has developed in collaboration with the Nexans company a Bi2212 wire having 18 sub-elements. The results of the critical current measurement are presented here and compared with already existing ribbons. The round wire has also been twisted to study twisting degradation.**

Index Terms—Bi2212/Ag superconducting wire and tape, critical current, High-temperature superconductors, Superconducting filaments and wires.

I. INTRODUCTION

Growing interest in research done under high magnetic field especially using NMR techniques are driving conditions to develop new HTS materials. As energy consumption is in the range of 1 MW/T above 20 T for the high field resistive magnets one can easily imagine the potential benefits of a fully superconducting high field magnet.

Despite a difficult heat treatment cycle to generate the superconducting phase Bi2212 [1]-[3] is one of the most promising candidates to generate high magnetic field. In order to design a high field magnet engineers need a superconducting material[4]-[5] that can be processed over long length and prefer a round shaped wire[6]-[7] enabling conventional cabling process[8]-[9] among other solutions.

CEA-Saclay and Cadarache started in 2005 with the Nexans company a R&D work to develop a Bi2212 round wire and compare its properties with already existing ribbons. In this paper the critical current measurements are presented for Bi2212 ribbons and round wire over the 0-15 T and 4.2-30 K range.

Manuscript received 19 August 2008. This work, supported by the European Communities under the contract of Association between EURATOM / CEA was carried out within the framework of the European Fusion Development Agreement. The views and opinions expressed herein do not necessarily reflect those of the European Commission.

Jean-Michel Rey, Lionel Quettier, Jean-Marc Gheller, Ronan Le Bouter, Daniel Tordera, Olivier Louchard are with the CEA-DSM-IRFU-Service des Accelerateurs de Cryogénie et Magnétisme, Centre d'études de Saclay, 91 191 Gif sur Yvette, France. corresponding author : J-M Rey phone: 33 1 69 08 66 85 fax: 33 1 69 08 69 29; e-mail: j-m.rey@cea.fr.

Jean-Luc Duchateau, is with the CEA-DSM-DRFC-Service Tokamak Exploitation et Pilotage, Centre d'étude de Cadarache, 13 108 Saint Paul lez Durance, France.

Arnaud Allais is with the Nexans Company, 4-10 rue Mozart, 92 587 Clichy Cedex, France.

II. SUPERCONDUCTING MATERIAL

A. Ribbon

Bi2212 ribbons received from Nexans came from two production batches supposedly identical. The main parameters of this ribbon are given in Table I. Originally this material has been developed for a SMES working at 20 K. The SMES has been built and successfully tested and an extensive bibliography is available on this subject [10]-[11].

B. Round wire

The round wire has been developed by CEA-IRFU as an internal R&D effort, in collaboration with the Nexans Company. This program started in 2005 was aimed to prepare cabling developments for high intensity variable fields magnets. Twisting the wires to study the influence of transposition pitch on the losses was one of the major objectives [12]. To limit the losses a design with small filaments and numerous sub-elements has been chosen. Parameters on this material can be found on Table I. More details on the superconducting ribbon and wire can be found on ref [12].

TABLE I RIBBON AND ROUND WIRE DATA.

	Unit	Ribbon	Round wire
Width	mm	4	
Thickness	mm	0.21	
Diameter	mm		0.8
Cross section	mm²	0.84	0.5
Number of filaments		76	666
Number of sub elements			18
SC cross section	mm²	0.21	0.053
SC / Non SC ratio	%	25 %	10.5 %

C. Heat treatment

In order to be tested the superconducting samples have first been reacted on Inconel mandrel at the nominal radius of the vamas testing support. During this heat treatment the Bi2212 ribbon is protected from the diffusion of foreign chemical species coming from the Inconel mandrel by a layer of nickel mesh. The heat treatment was adjusted to the chemical composition of each batch of superconducting materials. During the heat treatment the oxygen stiochiometry is established and the superconducting phase expands.

For the ribbon and the round wire the heat treatment was done by the Nexans Company, the wire has been later on transferred on titanium testing mandrels identical to the one used to test Nb_3Sn wires. During the heat treatment the outer shell of the wire sticks locally to the nickel mesh used to prevent diffusion from the inconel mandrel to the superconducting wire. Removing the wire from the mandrel should therefore be done very carefully.

D. Sample preparation.

Samples were tested on vamas like mandrels, adapted from the design of the testing samples used in Nb_3Sn development. After reaction the ribbons and wires are transferred from the reaction mandrel to the testing mandrel.

For the measurements on round wires only titanium alloy mandrels have been used.

For the strain dependence studies on ribbon other materials than the titanium alloy have been used to realize vamas mandrels. Some have been made in Copper, Stainless steel, Aluminum.

Fig. 1. Bi2212 ribbon on an adapted vamas mandrel.

III. TESTING DEVICE

The samples have been tested on the Cetacé test station, upgraded to allow critical current measurement at various temperatures ranging from 4.2 K to 30 K. Fig. 2 shows a view of this test station.

The variable temperature device has been designed using a two stage gas regulation concept. A first stage of thermal regulation is done outside the magnet using a dedicated helium evaporator. At that stage the helium gas is put at a temperature of 1 K lower than the test temperature. The second stage is achieved directly above the sample and the final gas temperature is adjusted with a precision better than 0.1 K. In order to reduce the heat losses near the sample the lower half of the current feed through are composed of copper and 4 ribbons of Bi2212 superconductor. This allows a current up to approximately 1000 A at 4.2 K to be put in the sample. The main cryostat contains a superconducting solenoid manufactured by Oxford Instrument. It produces 15 T at 4.2 K using a 100 A current. The field variation is 1T/min up to 15 T. The useful cold bore in the cryostat is 49 mm.

The voltage/current curve is recorded for each sample to identify the critical current. Two pairs of voltage taps are fitted on the superconducting wire, respectively with distances of 100 and 200 mm. The critical current Ic is defined as the current in the sample corresponding to a resistance of 1µV/cm the same value as the one used for low Tc superconductors.

Critical current measurement is made at 4.2 K; 10 K, 20 K and 30 K. The thermal stability during the tests is better than 0.5 K.

Fig. 2. The CETACE test station: on the right the helium tank with the gas exchanger on its top, in the middle the cryogenic insert, on the left the superconducting magnet.

IV. RIBBON MEASUREMENTS

A. Measurement scatter.

Critical current measured on samples coming from the same batch allowed to estimate the scatter within this production batch.

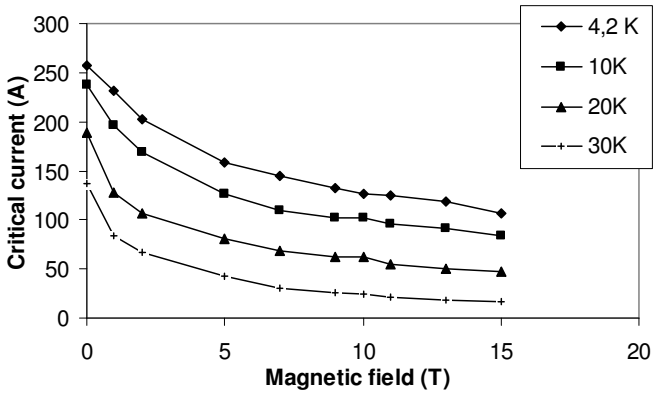

Fig. 3. : Mean values of the critical current measured on ribbons at T = 4.2, 10, 20 and 30 K.

The standard deviation within one material batch has been calculated as 11%, 10%, 15% and 30% for measurements

done respectively at 4.2 K, 10 K, 20 K and 30 K. The mean critical current values of these tests are given in Fig. 3.

B. Measurement reproducibility.

Some measurements have been performed on the same samples at several month intervals to check for changes in the critical current. It is surprising to state that the critical current of the ribbon increases during the second set of measure almost every time. This improvement of several percent in the superconducting properties was unexpected. An assumption to explain it is that the current flowing within the superconducting material helps the grain connectivity.

C. Material batch influence.

Some tests have been performed on samples from both batches of ribbons installed on mandrel of the same material to check for differences between material batches. A difference of 10% in the mean critical current value has been stated between both batches. Nevertheless normalizing the critical current with the critical current without field for both samples proved the superconducting material behaved the same way in both cases. This led us to conclude that one of the samples has apparently a lower superconducting content than the other.

D. Magnetic field and temperature dependence on Ic.

One of the ribbons has been extensively tested and the mean values of critical current over the tested samples are plotted on figure 3. Assuming the behavior in the 5 to 15 T area is linear enables to extrapolate the critical field value for each temperature. These are 35.6 T, 35.5 T, 28.2 T and 19.8 T respectively for 4.2 K, 10 K, 20 K and 30 K. These values are plotted on Fig. 14.

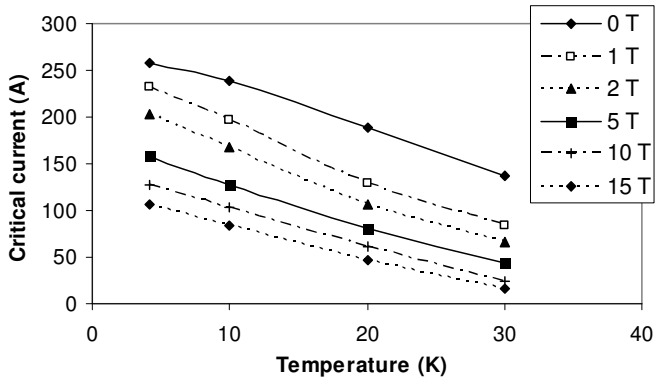

Fig. 4. : Critical current as function of temperature for different magnetic fields.

Plotting the values of critical current from Fig. 3 as a function of temperature gives Fig. 4. Approximating the curves of Fig. 4 with lines allows determining the slopes which varies from 4.7 A/K @ 0 T to 3.5 A/K @ 15 T. These lines intersect the temperature axis on points shown on Fig. 5, representing the critical temperature with respect to the magnetic field. The slope of the mean line of the critical temperature versus field between 1 and 15 T is 0.64 K/T, and the extrapolation gives a critical field of 60 T. Superconductivity appears at 85 K in Bi2212 with the disappearance of resistivity but current carrying capacity is effective at much lower temperature. This is the meaning of the critical temperature of 60 K appearing on fig 5 at 0 T. The drop in the 0-1 T area means that both grain orientation and inter-grain connectivity are strongly field dependant.

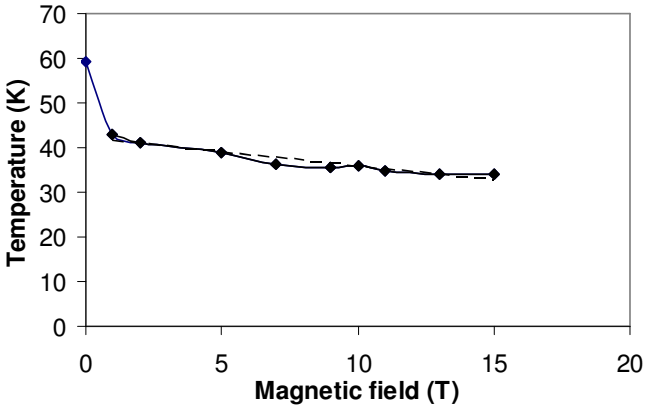

Fig. 5.: Critical temperature extrapolated from fig. 6 as function of magnetic field.

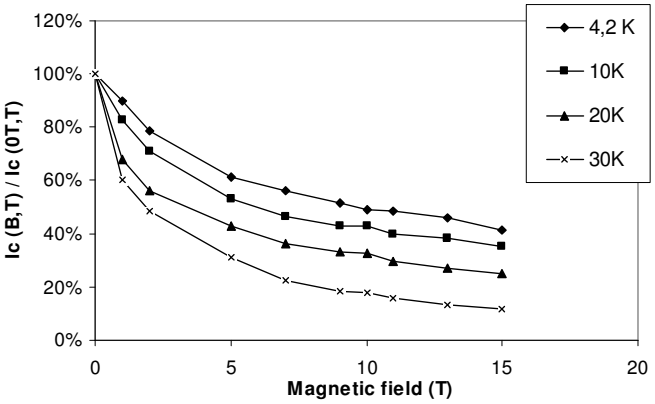

Fig. 6.: Mean values of the critical current at any field normalized to the critical current without magnetic field for tests performed on the ribbon at T = 4.2, 10, 20 and 30 K.

As the scatter between measurements from one sample to another is fairly large one can plot the critical current at any field normalized to the critical current without magnetic field as seen on Fig. 6. The discrepancy between the different samples is strongly reduced. This means that the critical current of one sample corresponds to the local value at the location of the largest defect in this sample. This is in agreement with the Weibull theory of ceramic materials.

V. ROUND WIRE MEASUREMENTS

Two heat treatments have been realized on this wire. The first with only bare wire and the second with all the twisted wires in the same batch and one untwisted reference wire. The critical current values of all the round wires tested at 4.2 K are shown in Fig. 7. Measurement scatter on the round wire is greater than 15% at 4.2 K. The critical current density of the best round wire sample is shown on Fig. 8.

The improvement in superconducting properties between

the first and second tests on the same sample has not been observed for the round wire.

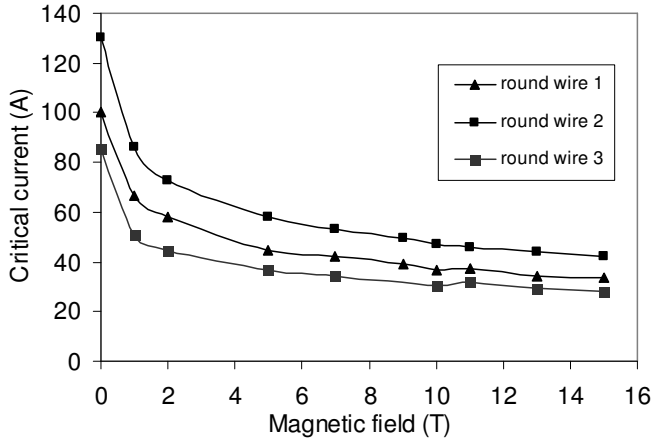

Fig. 7. : Critical current as a function of magnetic field for the different round wire samples tested at 4.2K.

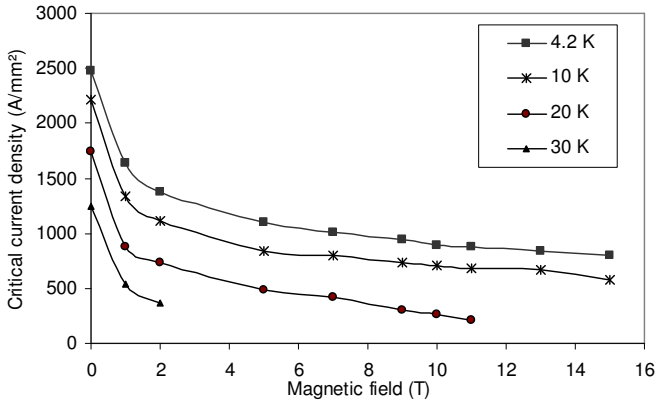

Fig. 8. : Critical current density for the best round wire sample tested.

As for tape the same normalizing exercise can be done for the round wire (Fig. 9.). Once again the curves become superimposed stating that the critical current reflects the cross section having the lowest superconducting material content.

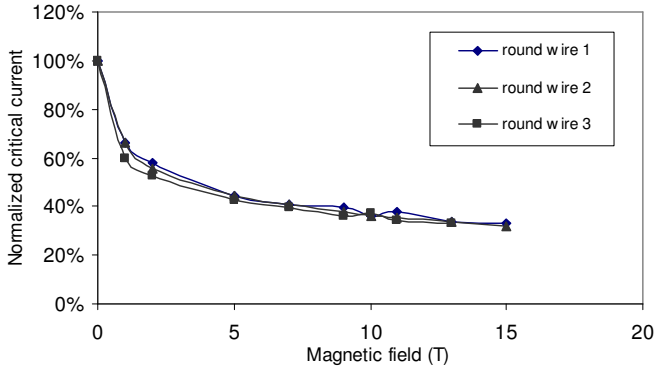

Fig. 9. Values of the critical current at any field normalised to the critical current without magnetic field for the 3 round wire samples tested at 4.2 K.

The critical current normalized to the critical current without magnetic field is shown on Fig. 10. The scatter between the points is greater than in the case of the ribbon. The drop in critical current between the 0 T and 1 T values confirms an effect of the ceramic structure on the critical current. The volume fraction of superconducting material well oriented with respect to the magnetic field is greater in the ribbon than in the round wire. Therefore the magnetic field has less influence on the ribbons properties than on the wire properties.

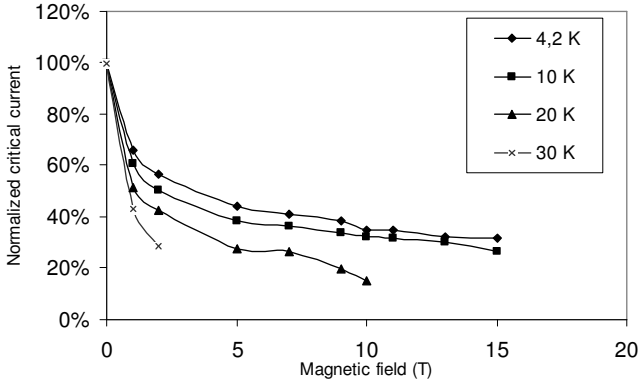

Fig. 10. Mean values of the critical current at any field normalized to the critical current without magnetic field for tests performed on the round wire at T = 4.2, 10, 20 and 30 K.

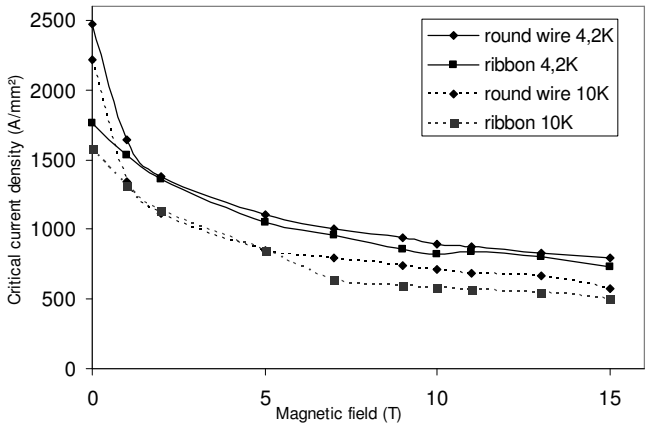

Fig. 11. : Comparison of critical current density measured on ribbon and round wire as a function of magnetic field.

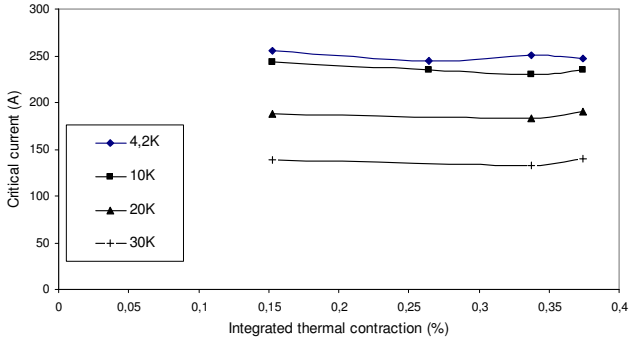

Fig. 12. : Critical current plotted as a function of the integrated thermal contraction of the mandrel material. Points corresponds to measurements on titanium mandrel (integrated thermal expansion 0.159%) stainless steel (ITC 0.26%) Copper (ITC 0.34%) Aluminum (ITC 0.37%).

Comparing critical current density of ribbon and round wire is made on Fig. 11. In the absence of magnetic field the superconducting properties are better on round wire than on ribbon. Other publications have stated that as well [13].

Using measurement mandrels of different materials namely copper aluminum alloy and stainless steel was intended to provide information about strain influence on critical current. As can be stated on Fig. 12 the critical current is not affected

by the mandrel integrated thermal contraction. This is in agreement with other published data [14].

VI. Model Development

Magnet designers always dream of having simple laws to estimate superconducting properties of their conductors based on a reduced number of simple experimental measurements.

In order to predict critical current values we decided to develop a model based on the knowledge of critical current without field. As the effective cross section of superconducting material is uneasy to estimate after heat treatment reaction the use of critical current density does not seems to be appropriate. Plotting the critical current without magnetic field normalized to its value at 4.2 K versus temperature shows a linear behavior. The points on Fig. 13 come from different samples ribbons and round wire and follow the same following fit:

$$I_c(T, B = 0T) = -0.0189\,T + 1.0894$$

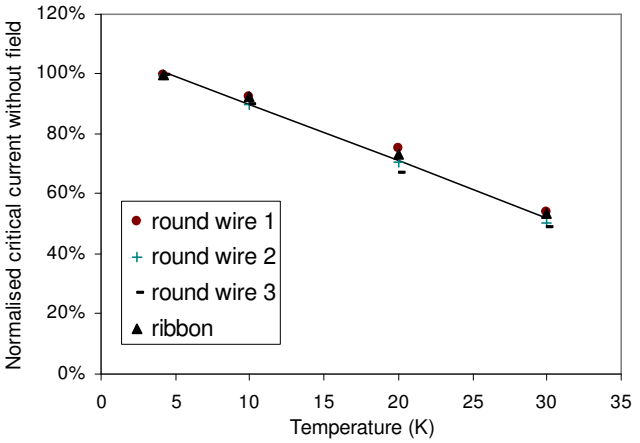

Fig. 13. : Critical current without magnetic field normalized to the critical current at 4.2 K without field plotted versus temperature.

This equation represents an intrinsic parameter (not shape dependant) of the superconducting material, like the critical field plotted on Fig. 14 using the data extrapolated from Fig. 3. The critical field approximation follows the fit:

$$B_c(T) = -0.0188\,T^2 + 0.0033\,T + 36.392$$

The type of formula chosen for the critical current model comes from diffusion process. The following formula proved to be effective with the set of parameters given in Table II.

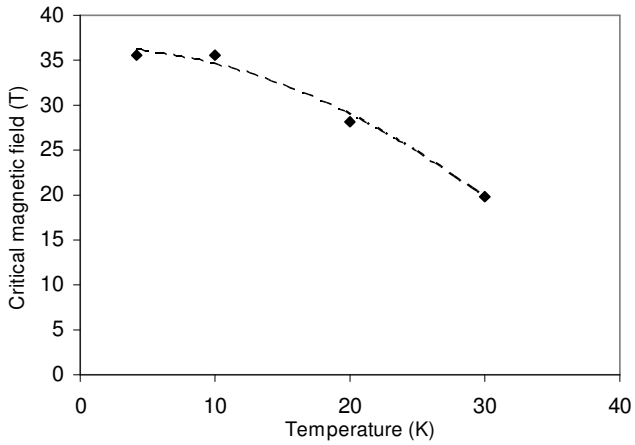

Fig. 14. : Critical magnetic field versus temperature.

$$I_c = I_c(T, B = 0T)\,\exp(-KA^n C^m)$$

With: $A = B/(B_c(T) - B)$

$C = T/(T_c - T)$

TABLE II Parameters used in the model

Symbol	Ribbon	Round wire
K	2	2.5
n	0.45	0.3
m	0.25	0.27

Using the parameters of Table II the critical current versus magnetic field is plotted for ribbon on Fig. 14 and for round wire on Fig. 15 and compared with the experimental points coming from Fig. 3 and values measured on round wires.

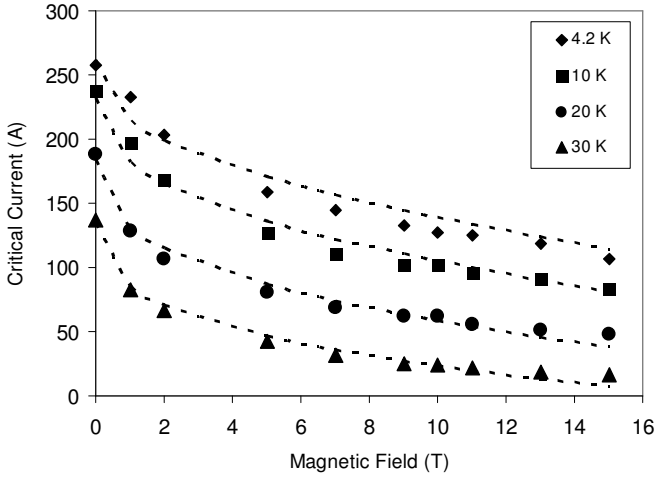

Fig. 15. : Critical current lines at various temperature obtained from model calculation compared with experimental points measured on ribbon as a function of magnetic field.

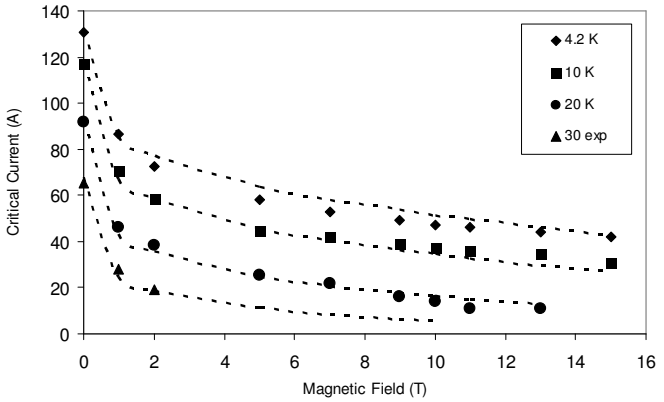

Fig. 16. : Critical current lines at various temperature obtained from model calculation compared with experimental points measured on round wire as a function of magnetic field.

VII. Conclusion

A new Bi2212 round wire has been produced tested and compared to existing Bi2212 ribbon. Its critical current density at low field is higher than the one of the ribbon. At medium to high induction the critical current density are equivalent. Normalized critical current for round wire and ribbon are different. This difference is attributed to conductor shape and its influence on superconducting crystal orientation. For both conductors the overall properties reflects the behavior of the location having the lowest superconductor cross section or the largest local defect.

An empirical model has been developed to calculate the critical current as a function of temperature and magnetic field using 3 parameters and 2 experimental fits for the critical magnetic field and the critical current without field. These two equations reflect intrinsic properties of the Bi2212 superconductor and we suppose the 3 parameters are shape and process dependant.

References

[1] D.E Wiesolowski et al, “Reactions between oxides and Ag-sheated $Bi_2Sr_2CaCu_2O_x$ conductors”, Supercond. Sci. technol. 18 (2005) R934-R943

[2] T. Koizumi et al,.”Bi-2212 Phase formation process in multifilamentary Bi-2212/Ag wires and tapes”Applied Superconductivity, IEEE Transactions on, Volume 15, Issue 2, June 2005, Page(s): 2538-2541

[3] Nakane, T.; Isobe, M.; Mochiku, T.; Matsumoto, A.; Kitaguchi, H.; Kumakura, H.; “Effect of high oxygen pressure post-annealing on the J/sub c/-B characteristics of Bi-2212/Ag tapes” Applied Superconductivity, IEEE Transactions on, Volume 15, Issue 2, Part 3, June 2005 Page(s):2542 – 2545

[4] Kim, S.-C.; Ha, D.-W.; Han, I.-Y.; Oh, J.-G.; Lee, J.-H.; Oh, S.-S.; Ha, H.-S.; Song, K.-J.; Sohn, “Effect of filament configuration on critical current density of Bi-2212/Ag wires with low Ag ratio” Applied Superconductivity, IEEE Transactions on, Volume 18, Issue 2, June 2008 Page(s):1188 – 1191

[5] Holesinger, T.G.; Kennison, J.A.; Marken, K.R.; Hanping Miao; Meinesz, M.; Campbell, S.; “Compositional and microstructural analysis of high I/sub c/ and J/sub c/ Bi-2212 conductors” Applied Superconductivity, IEEE Transactions on, Volume 15, Issue 2, Part 3, June 2005 Page(s):2562 – 2565

[6] Hanping Miao; Marken, K.R.; Meinesz, M.; Czabaj, B.; Seung Hong; “Development of round multifilament Bi-2212/Ag wires for high field magnet applications” Applied Superconductivity, IEEE Transactions on, Volume 15, Issue 2, Part 3, June 2005 Page(s):2554 – 2557

[7] Marken, K.R., Jr.; Miao, H.; Meinesz, M.; Czabaj, B.; Hong, S.; “Progress in Bi-2212 Wires for High Magnetic Field Applications” Applied Superconductivity, IEEE Transactions on, Volume 16, Issue 2, June 2006 Page(s):992 – 995

[8] Ha, D.-W.; Kim, S.-C.; Han, I.-Y.; Oh, J.-G.; Lee, J.-H.; Oh, S.-S.; Ha, H.-S.; Song, K.-J.; Sohn, M.-H.; Ko, R.-K.; Kim, H.-S.; Kim, T.-K.; “Study on Bi-2212 Rutherford Cabling Process for SMES” Applied Superconductivity, IEEE Transactions on Volume 18, Issue 2, June 2008 Page(s):1192 – 1195

[9] Dong-Woo Ha; Sang-Cheol Kim; Jae-Gun Oh; Hong-Soo Ha; Nam-Jin Lee; Kyu-Jeong Song; Tae-Hyung Kim; Rock-Kil Ko; Ho-Sup Kim; Seong-Kuk Park; Sang-Kil Lee; Yu-Mi Roh; Sang-Soo Oh; “Influence of Filament Number on Workability and Critical Current Density of Bi-2212/Ag Superconducting Wires” Applied Superconductivity, IEEE Transactions on, Volume 17, Issue 2, Part 3, June 2007 Page(s):3099 – 3102

[10] P. Tixador, B. Bellin, M. Deleglise, J. C. Vallier, C. E. Bruzek, A. Allais, and J. M. Saugrain “Design and First Tests of a 800 kJ HTS SMES”, Applied Superconductivity, IEEE Transactions on, Vol. 17, No. 2, June 2007, pp. 1967-1972.

[11] P. Tixador, M. Deleglise, A. Badel, K. Berger, B. Bellin, J. C. Vallier, A. Allais, and C. E. Bruzek “First Tests of a 800 kJ HTS SMES”, Applied Superconductivity, IEEE Transactions on, Vol. 18, No. 2, June 2008, pp. 774-778.

[12] Jean-Michel Rey, Lionel Quettier, Arnaud Allais, Hervé Cloez, Jean-Luc Duchateau, Jean-Louis Marechal, Louis Zani, Sylvain Girard, “Losses measurement in HTc Bi2212 ribbons and round wires“, Presented at ASC 2008 Chicago.

[13] Hanping Miao; Marken, K.R.; Meinesz, M.; Czabaj, B.; Seung Hong; Twin, A.; Noonan, P.; Trociewitz, U.P.; Schwartz, J.; “High Field Insert Coils From Bi-2212/Ag Round Wires” Applied Superconductivity, IEEE Transactions on, Volume 17, Issue 2, Part 2, June 2007 Page(s):2262 – 2265

[14] Bennie ten Haken, Herman H. J. ten Kate, “Compressive and tensile axial strain reduced critical currents in Bi-2212 conductors” Applied Superconductivity, IEEE Transactions on, Volume 5, Issue 2, No 2, June 1995 Page(s):1298 – 1301.